sustainability

MDPI

Article

A Physics-Based Algorithm for Dynamic CO_2 Emissions Estimation in Demand-Responsive Transport and Ride-Hailing Services

Cătălin Beguni [1,2], Alin-Mihai Căilean [1,2,*], Eduard Zadobrischi [1,2], Sebastian-Andrei Avătămăniței [2], Alexandru Lavric [1,2] and Florinel-Mădălin Stoian [3]

[1] Department of Computers, Electronics and Automation, Stefan cel Mare University of Suceava, 720229 Suceava, Romania; catalin.beguni@usm.ro (C.B.); eduard.zadobrischi@usm.ro (E.Z.); lavric@usm.ro (A.L.)
[2] Integrated Center for Research, Development and Innovation in Advanced Materials, Nanotechnologies and Distributed Systems for Fabrication and Control, Stefan cel Mare University of Suceava, 720229 Suceava, Romania; sebastian.avatamanitei@usm.ro
[3] Proptech Industry, 230047 Slatina, Romania; florinstoian2003@gmail.com
* Correspondence: alinc@eed.usv.ro

Abstract

As road transport is a major contributor to anthropogenic CO_2 emissions, the importance of sustainable mobility planning and fleet management becomes very clear. Therefore, this article proposes a physics-based mathematical framework for dynamic estimation of CO_2 emissions. The proposed framework is very flexible and enables CO_2 assessment for different types of vehicles (i.e., combustion engine and electric vehicles), traffic and operating conditions. The proposed software prototype is evaluated through representative urban and peri-urban simulation scenarios. These scenarios involve conventional public transport, private vehicles, and demand-responsive ride-hailing services. The simulation results show that vehicle occupancy is one of the main factors impacting specific CO_2 emissions. In this context, in low-passenger-demand and dispersed travel conditions, demand-responsive mobility services can achieve lower emissions per passenger-kilometer than conventional public transport. In contrast, when occupancy levels are sufficiently high, public transport remains the most efficient option. These results indicate that there is no universally optimal transport mode and that emission efficiency is the result of a matching between vehicle capacity and passenger demand. Therefore, the proposed framework delivers a transparent and practical decision-support tool for transport mobility services.

Keywords: carbon emissions; carbon footprint; ride-hailing; on-demand mobility; public transport; peri-urban mobility; sustainable transportation; comparative assessment; environmental impact

Check for updates

Academic Editors: Yi Li, Meng Meng and Ziyue Yuan

Received: 16 July 2026
Revised: 7 August 2026
Accepted: 13 August 2026
Published: 13 August 2026

Copyright: © 2026 by the authors. Licensee MDPI, Basel, Switzerland. This article is an open access article distributed under the terms and conditions of the Creative Commons Attribution (CC BY) license.

1. Introduction

Road transportation represents the backbone of modern society, facilitating the movement of people and goods and contributing to economic development and well-being [1,2]. Nevertheless, despite enormous benefits, road transportation also generates important challenges. On the one hand, road transportation affects everyday life through road traffic accidents and the associated injuries, fatalities and financial costs [3]. On the other hand, according to existing estimations, road transportation is one of the main sources of greenhouse gas emissions, accounting for a significant share of anthropogenic CO_2

emissions [4–12]. The continuous growth of the vehicle fleet, the fast urbanization and the dependence on private vehicles indicate that this sector has an important role to play in the transition toward lower CO_2 emissions [9–12]. Within this context, ride-hailing services have emerged as an important topic of research because of their growing role in urban transportation and their potential to contribute to road transport decarbonization [13,14]. Therefore, several studies have analyzed modal shift and competition between ride-hailing and public transit [15–17]. Nevertheless, there is no consensus in the literature reviewed on the effects of ride-hailing on emissions. Many studies report mixed or context-dependent findings, depending on factors such as congestion and urban density [18,19].

To the authors' knowledge, few simulation-based studies explicitly compare CO_2 emissions across transport modes under identical and non-ideal traffic conditions. In many cities, ride-hailing has led to a decrease in public transit use, suggesting that this alternative can, in some cases, lead to an increase in total emissions. This effect is caused by the absence of an efficient pooling system, which in turn leads to vehicles that travel without passengers between orders [20,21]. In this context, it would be useful to assess the impact of CO_2 emissions generated by vehicles not only at the macro-level (i.e., national or European), but also at the micro-level [22]. Such an approach would enable a better management of transport-related CO_2 emissions for individual users, companies with car fleets, local authorities, or mobility service providers. Additionally, the availability of tools that provide rapid, clear and comparable assessments of these emissions, adapted to real conditions of use, can enable better fleet management decisions. In this regard, such tools can support decision-making regarding the choice of vehicle type (i.e., petrol, diesel, electric), fleet sizing, or route selection and planning. Moreover, micro-level CO_2 assessment can be used in dynamic urban mobility policies and can contribute to the effectiveness of the public transportation.

Existing models are often rather complex, difficult to use, and dependent on data sets that are not available for independent final users (i.e., drivers or managers of small vehicle fleets). On the other hand, basic indicators such as those provided by car manufacturers (i.e., average fuel consumption) do not reflect the impact of real traffic conditions, driving style or route type [23]. Therefore, developing a simplified but physically grounded mathematical emission monitoring tool represents a relevant direction of research. Such an instrument can be used for realistic assessments concerning the climate impact of road travel. Moreover, as the tool does not require complex measurement infrastructure, it can be implemented at the micro-level, serving in providing decision support for individual drivers and for small-fleet managers. Thus, this article proposes a simplified model for CO_2 estimation in small vehicle fleets. The model is intended to be used within the RINO platform, a new on-demand transport platform which is under development and which is scheduled for market launch in early 2027. Subsequently, in order to demonstrate its performance, the CO_2 estimation tool is used to evaluate the impact for different types of vehicles, in different traffic conditions, with different driving styles and in different occupancy conditions. The proposed model allows for dynamic emission estimates for each scenario, rather than only average values. Moreover, the framework also enables explicit comparisons between transport modes under similar traffic conditions and calculating emissions per passenger-kilometer, which is essential for comparisons between public transport and demand-driven alternatives. The model, being deterministic and dynamic, extends existing approaches by offering the capability to quantify specific situations (e.g., peri-urban), not just broad urban environments.

The contribution of the present work consists of integrating well-established longitudinal vehicle dynamics equations within a transparent and low-computational framework that combines route-dependent vehicle dynamics, Internal Combustion Engine Vehicle

(ICEV) and Electrical Vehicle (EV) energy consumption, regenerative braking, idling and auxiliary consumption, CO_2 emission factors, vehicle occupancy and passenger-kilometer indicators for comparative mobility assessment. While models designed for detailed emission inventories and large-scale evaluations such as Motor Vehicle Emission Simulator (MOVES) and Handbook Emission Factors for Road Transport supported by Passenger Car and Heavy-Duty Employment Model (HBEFA/PHEM) provide more detailed and extensively calibrated emission modeling capabilities, the proposed approach is intended as a simplified computational methodology for small-fleet management and on-demand mobility applications. This simplification incurs an inevitable trade-off between model fidelity and computational and data requirements. Therefore, the present framework should be regarded as a comparative assessment tool rather than a substitute for experimentally calibrated comprehensive emission models.

Overall, this article focuses on a real need for a practical and transparent approach that enables CO_2 emissions estimation at the micro level. The proposed algorithm is based on a simplified mathematical model that is suitable for real-world transport applications. Unlike existing approaches that rely on extensive datasets or complex simulation frameworks, the model proposed in this work is designed to provide dynamic, scenario-specific emission estimates that consider different traffic conditions, different vehicle types and different occupancy levels. As a result, the proposed methodology enables reliable comparisons between transport alternatives and supports decision-making in small-fleet management and on-demand mobility services. Therefore, the proposed approach aims to bridge the gap between theoretical emission estimation methods and practical implementation in real-world transport planning.

The rest of this article is structured as follows. Section 2 offers a detailed presentation of the mathematical model used in the simulations. Next, Section 3 provides the simulation scenarios considered and the results. Finally, Section 4 discusses the implications of the proposed approach, its potential applications in fleet management and concludes the article.

2. Model Presentation and Its Software Implementation

The proposed simulation model is based on a detailed physically based mathematical model of vehicle dynamics and energy balance, which integrates resistance forces and energy requirements along a discretized route using discrete time steps. This approach enables the estimation of energy consumption and CO_2 emissions for different vehicle types, namely ICEVs and EVs, in various traffic scenarios.

2.1. Theoretical Mathematical Model for CO_2 Emissions

The forces acting on the vehicle are assumed to be collinear with the direction of motion, while lateral effects are neglected. This simplification is consistent with the primary objective of the proposed framework, namely the estimation of route-level CO_2 emissions using a computationally efficient and physically transparent model. The dominant contributors to vehicle energy demand are represented through longitudinal dynamics, while lateral effects such as cornering resistance and tire slip are intentionally neglected. Experimental studies [24] have shown that cornering-related energy losses typically account for approximately 3.1% of the total vehicle energy consumption and may increase to about 5.8% only for highly curved urban routes. Therefore, although these effects can become relevant in detailed vehicle dynamics analyses, their influence is generally secondary for the comparative transport scenarios investigated in this work. Future developments of the proposed framework may incorporate lateral dynamics for applications requiring higher modeling fidelity. Another important note is that during periods when $v(t) = 0$, even if the power at the wheels is zero, an ICEV may still consume fuel while idling. This phe-

nomenon can be modeled separately. Based on these assumptions, the simulation for a vehicle traversing a route over the time interval t ∈ [0, T] uses the parameters presented in Table 1.

Table 1. Categories of input data parameters.

Input Data Categories	Parameters	Definition
Route data	t_i	discrete time vector (s)
	s	road slope
	θ	road slope angle (degree)
	v_{thr}	stopping threshold speed (m/s)
	d	distance traveled (m)
	$v(t) = dd(t)/dt$	vehicle velocity (m/s)
	$a(t) = dv(t)/dt$	vehicle acceleration (m/s^2)
	g	gravitational acceleration (m/s^2)
	ρ	air density (kg/m^3)
	Δt	time interval (s)
Traffic	*Scenario A*	dense urban/heavy-traffic condition and uncovered by ride-hailing platforms
	Scenario B	peri-urban/light-traffic condition and uncovered by ride-hailing platforms
	Scenario C	dense urban/heavy-traffic condition and covered by ride-hailing platforms
	Scenario D	peri-urban/light-traffic condition and covered by ride-hailing platforms
Energy	*LHV*	lower heating value of fuel (J/kg)
	ε_{fuel}	fuel CO_2 emissions factor (g CO_2/kg fuel)
	ε_{elec}	electricity CO_2 emissions factor (g CO_2/kWh)
	η_{ICEV}/η_{EV}	effective average powertrain efficiency
	η_{regen}	regenerative braking efficiency ($0 \leq \eta_{regen} \leq 1$)
	P_{aux}	Average auxiliary power (W)
Vehicle	m	vehicle effective mass (kg)
	C_d	aerodynamic drag coefficient
	A	maximum frontal area (m^2)
	C_{rr}	rolling resistance coefficient

The longitudinal force at the wheels is the model's fundamental equation and is determined by the sum of inertia, gravitational, rolling resistance, and aerodynamic drag components [25]:

$$F_{tot}(t) = m \cdot a(t) + m \cdot g \cdot sin\theta(t) + C_{rr} \cdot m \cdot g \cdot cos\theta(t) + \frac{1}{2} \cdot \rho \cdot C_d \cdot A \cdot v^2(t). \quad (1)$$

For small slopes, frequently used in road applications, the following approximations are adopted:

$$sin\theta(t) \approx \frac{s(t)}{100}, cos\theta(t) \approx 1, \quad (2)$$

where $s(t)$ is the slope expressed as a percentage. Instantaneous mechanical power at wheels is defined as the product of total longitudinal force and the speed of the vehicle:

$$p_w(t) = F_{tot}(t) \cdot v(t). \tag{3}$$

The following relations can be written for traction and braking power:

$$p_{w^+}(t) = max(p_w(t), 0), \tag{4}$$

$$p_{w^-}(t) = max(-p_w(t), 0). \tag{5}$$

The operator $max(\cdot, 0)$ is used because during deceleration $p_w(t)$ can become negative, and negative power does not represent additional mechanical consumption, but rather energy that must be dissipated or recovered.

The required energy and the mechanical energy available during deceleration (potentially recoverable) can be expressed by:

$$E_{req} = \int_0^T p_{w^+}(t)dt, \tag{6}$$

$$E_{neg} = \int_0^T p_{w^-}(t)dt, \tag{7}$$

where T is the total travel duration. These quantities form the basis for the calculation of energy consumption and for modeling energy recovery in electric vehicles.

To establish a direct relationship between mechanical power and consumption, instantaneous power flow rates are defined:

$$\dot{m}_{fuel}(t) = p_{w^+ICEV}(t)/(\eta_{ICEV} \cdot LHV), \tag{8}$$

$$\dot{e}_{bat}(t) = p_{w^+EV}(t)/\eta_{EV}, \tag{9}$$

where $\dot{m}_{fuel}$ is fuel mass flow rate (kg/s), and $\dot{e}_{bat}$ is the electrical power flow rate (W).

The consumption rate for an ICEV is defined by:

$$E_{fuel} = E_{req-ICEV}/\eta_{ICEV} + E_{idle}, \tag{10}$$

$$m_{fuel} = E_{fuel}/LHV. \tag{11}$$

For an EV, the battery consumption (E_{bat}) can be defined as:

$$E_{bat} = E_{bat-tract} + E_{bat-aux} - E_{regen}, \tag{12}$$

where:

$$E_{bat-tract} = E_{req-EV}/\eta_{EV}, \tag{13}$$

$$E_{regen} = \eta_{regen} \cdot E_{neg}. \tag{14}$$

No significant traction energy is consumed in an electric vehicle when it is stationary, however auxiliary consumers may continue to draw energy. This aspect is covered by the $E_{bat\text{-}aux}$ term. Auxiliary power is modeled explicitly only for electric vehicles. For ICEVs, the η_{ICEV} term is interpreted as an effective average powertrain efficiency that implicitly accounts for average auxiliary and parasitic losses [26]. Also, idling consumption can be relevant where congestion occurs. A simple representation uses a constant mass flow rate

(kg/s), which can be converted into volumetric consumption (l/h) knowing the fuel density. If the total stop duration t_{stop} is known, then:

$$m_{fuel-idle} = \dot{m}_{idle} \cdot t_{stop}, \tag{15}$$

and associated energy would be:

$$E_{idle} = m_{fuel-idle} \cdot LHV. \tag{16}$$

In practice, t_{stop} can be extracted from the $v(t)$ profile by detecting the intervals where $v(t)$ is below a small threshold (for example, 0.5 m/s). Equation (15) represents a simplified engineering approximation in which idle fuel consumption is assumed constant throughout the stop period. The present model does not explicitly represent transient engine thermal management strategies, nor automatic start–stop systems, which could improve the efficiency with 3 to 4% in the summer period [27]. Consequently, vehicles equipped with start–stop technology are conservatively modeled as conventional internal combustion vehicles operating continuously during idle periods. This simplification was adopted to preserve the transparency and computational efficiency of the proposed framework, while recognizing that more detailed engine operating models could further improve estimation accuracy.

To calculate CO_2 emissions, the model considers the Well-to-Wheel (W2W) assessment, which refers to the full life cycle emissions from fuel or energy production through final use at the wheels. It is the sum of Well-to-Tank (W2T) assessment, which refers to emissions from extraction, refining, production, transport, and distribution of the fuel or electricity, and Tank-to-Wheel (T2W) assessment, which refers to the emissions that occur when fuel is used to power the vehicle.

For an ICEV:

$$CO2_{ICEV-T2W} = m_{fuel} \cdot \varepsilon_{fuel}. \tag{17}$$

An additional upstream chain factor for W2T, denoted k_{W2T}, can be included, such that:

$$CO2_{ICEV-W2W} = CO2_{ICEV-T2W}(1 + k_{W2T}). \tag{18}$$

For an EV:

$$CO2_{EV-T2W} \approx 0. \tag{19}$$

$$CO2_{EV-W2W} = \mathrm{E}_{bat} \cdot \varepsilon_{elec}. \tag{20}$$

These formulations enable consistent comparisons between technologies within the same tool, with transparent assumptions about the emission factors.

In the case of passenger transport, assuming that N_p is the average number of passengers, one can determine the CO_2 emission per passenger-kilometer based on the total distance traveled, D. Accordingly, the following expression is obtained:

$$D = d(T) - d(0). \tag{21}$$

We define specific indicators for CO_2 emission per route:

$$e_{CO_2ICEV/km} = \frac{CO2_{ICEV-W2W}}{D} \cdot 10^3, \tag{22}$$

$$e_{CO_2EV/km} = \frac{CO2_{EV-W2W}}{D} \cdot 10^3. \tag{23}$$

Other indicators for passenger-kilometer emissions determination can be written as:

$$e_{CO_2ICEV/pkm} = \frac{CO2_{ICEV-W2W}}{D \cdot N_p} \cdot 10^3, \quad (24)$$

$$e_{CO_2EV/pkm} = \frac{CO2_{EV-W2W}}{D \cdot N_p} \cdot 10^3, \quad (25)$$

where $CO2_{ICEV\text{-}W2W}$ and $CO2_{EV\text{-}W2W}$ are expressed in g CO_2, D is expressed in meters, and the results, $e_{CO2ICEV}$ and e_{CO2EV}, are expressed in g CO_2/passenger-km.

2.2. Numerical Discretization

After the mathematical formalization of the model in the previous section, the next step is to translate the determined relations into a discrete numerical algorithm that can be implemented in a software prototype. The purpose of this step is not for an optimization, but rather to obtain a coherent and traceable implementation that respects the mathematical structure of the model. The algorithmic implementation must maintain a direct correspondence between the theoretical equations and the calculation steps, so that each numerical result can be justified by a well-defined mathematical relationship.

In order to do this, the simulation interval [0, T] is divided into n equal time steps of duration Δt. The dynamic variables are evaluated at each step i, corresponding to the time instant:

$$t_i = \mathrm{i} \cdot \Delta \mathrm{t}. \quad (26)$$

For numerical implementation of a dynamic model, the speed profile is discretized over these time intervals, yielding the following samples:

$$v_i = v(i \cdot \Delta t). \quad (27)$$

The acceleration can be approximated using finite differences:

$$a_i \approx (v_i - v_{i-1})/\Delta t. \quad (28)$$

The speed profiles employed in the simulations are predefined numerical trajectories sampled at a constant time interval and therefore do not contain measurement noise. Consequently, the finite-difference approximation of acceleration can be applied directly without additional filtering. In future implementations using real GPS or CAN-derived trajectories, appropriate signal preprocessing (e.g., smoothing or resampling) must be introduced prior to numerical differentiation in order to reduce noise amplification and improve acceleration estimation [28].

The road grade may be introduced through a series of either a slope value s_i expressed in percent or a slope angle θ_i expressed in radians. Forces are computed at each step i, and based on Equation (3), the power at the wheels is:

$$p_{w,i} = F_{tot,i} \cdot v_i, \quad (29)$$

where $F_{tot,i}$ represents the total tractive force at step i. Energies are obtained by summation (rectangular integration):

$$E_{req} \approx \sum max(p_{w,i}, 0) \cdot \Delta t, \quad (30)$$

$$E_{neg} \approx \sum max(-p_{w,i}, 0) \cdot \Delta t. \quad (31)$$

The stop time is estimated as:

$$t_{stop} \approx \sum I(v_i < v_{thr}) \cdot \Delta t, \tag{32}$$

where $I(\cdot)$ is the indicator function (1 if the condition is true, 0 otherwise), and v_{thr} is the threshold speed defining a stop. This discretization scheme is sufficiently robust and appropriate for prototype implementations.

2.3. Software Implementation and Algorithmic Structure

The software prototype, implemented in Python 3.9.6, allows experimentation with real-world parameters and the automatic generation of numerical and visual results, including the export of CSV files for post-processing analysis and comparative plots for specific emissions per distance and per passenger-kilometer. The algorithm is organized modularly, following the logical chain described below and illustrated in Figure 1: Input data → Preprocessing → Dynamic calculation over the time interval → Emissions calculation → Final indicators. This structure directly reflects the stages of the mathematical model presented and allows both detailed simulations based on complete speed profiles and simplified scenario analyses.

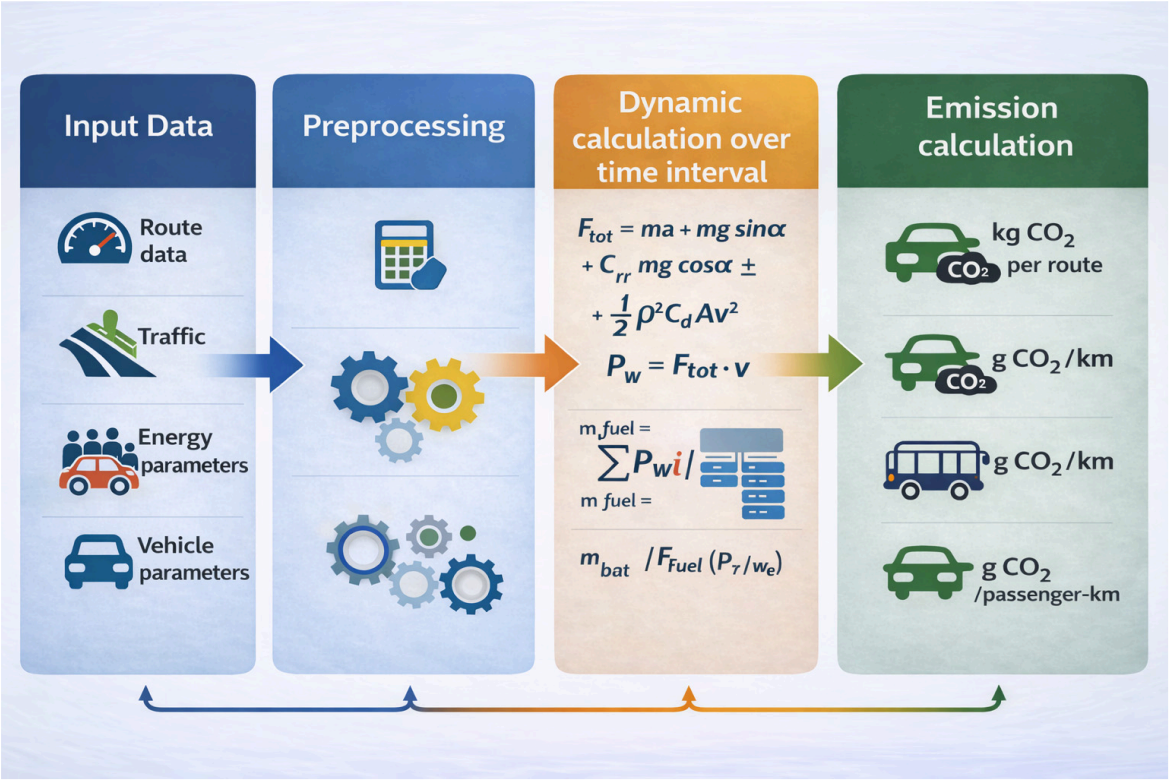


Figure 1. Data processing workflow for CO_2 emissions estimation.

At initialization, all cumulative energy quantities and stop time are set to zero:

$$E_{req} = 0,\ E_{neg} = 0,\ t_{stop} = 0. \tag{33}$$

Using these initial conditions together with Equations (18) and (20), the following results are obtained:

$$e_{CO_2 ICEV/km} = ((\sum max(m \cdot v_i \cdot (v_i - v_{i-1}) + m \cdot v_i \cdot g \cdot \frac{s_i}{100} \cdot \Delta t + C_{rr} \cdot m \cdot v_i \cdot g \cdot \Delta t + \\ + \frac{1}{2} \cdot \rho \cdot C_d \cdot A \cdot v_i^3 \cdot \Delta t, 0)) / (\eta_{ICEV} \cdot LHV) + \dot{m}_{idle} \cdot \sum I(v_i < v_{thr}) \cdot \Delta t) \cdot \frac{\varepsilon_{fuel} \cdot (1 + k_{W2T})}{D} \cdot 10^3. \tag{34}$$

$$e_{CO_2ICEV/pkm} = e_{CO_2ICEV/km}/N_p. \tag{35}$$

$$\begin{aligned} e_{CO_2EV/km} = ((\sum max(m \cdot v_i \cdot (v_i - v_{i-1}) + m \cdot v_i \cdot g \cdot \frac{s_i}{100} \cdot \Delta t + C_{rr} \cdot m \cdot v_i \cdot g \cdot \Delta t + \\ + \frac{1}{2} \cdot \rho \cdot C_d \cdot A \cdot v_i^3 \cdot \Delta t, 0)/\eta_{EV} - \eta_{regen} \cdot \sum max(-(m \cdot v_i \cdot (v_i - v_{i-1}) + m \cdot v_i \cdot g \cdot \frac{s_i}{100} \cdot \Delta t + \\ + C_{rr} \cdot m \cdot v_i \cdot g \cdot \Delta t + \frac{1}{2} \cdot \rho \cdot C_d \cdot A \cdot v_i^3 \cdot \Delta t), 0) + P_{aux} \cdot T) \cdot \frac{\varepsilon_{elec}}{3.6 \cdot 10^3 \cdot D}. \end{aligned} \tag{36}$$

$$e_{CO_2EV/pkm} = e_{CO_2EV/km}/N_p. \tag{37}$$

Because distance D is expressed in meters, both Equations (34) and (36) include the factor 10^3 in the numerator for meter-to-kilometer conversion. Equation (36) also includes the additional factor 3.6×10^6 in the denominator, which converts electrical energy from joules to kilowatt-hours, ensuring consistency with the units of the electricity emission factor ε_{elec} (g CO_2/kWh).

The proposed algorithm has been designed to support future calibration and validation against experimental or operational data. Once these stages are completed for a given application, the framework can be used to perform a wide range of analyses under different transport scenarios.

3. Simulation Scenarios and Results

This section presents the simulation scenarios considered in this study together with the corresponding results. The purpose is to demonstrate the applicability of the proposed CO_2 estimation model under representative operating conditions. The simulation scenarios consider different traffic environments, vehicle categories, occupancy levels, and mobility strategies. The results provide a comparative evaluation of the environmental performance of ride-hailing services and conventional public transport under the modelling assumptions adopted. The prototype, developed in Python 3.9.6, is intended to demonstrate the complete workflow of the proposed methodology. The required inputs consist of vehicle parameters, route characteristics, traffic scenario parameters, and speed–time profiles. The software processes the input data to estimate energy consumption and W2W CO_2 emissions, and generates comparative indicators, graphical visualizations, and CSV files for further analysis. The current implementation constitutes the computational core of the future RINO platform, where these functions are intended to be integrated with operational vehicle and route information to support fleet-management decision-making.

3.1. Defining Simulation Scenarios

As illustrated in Figure 2, the simulations are performed for the following representative scenarios: (i) dense urban/heavy-traffic condition and where ride-hailing services are not available; (ii) peri-urban/light-traffic condition and where ride-hailing services are not available; (iii) dense urban/heavy-traffic condition and with ride-hailing services; (iv) peri-urban/light-traffic condition and with ride-hailing services.

The vehicle parameters used in the simulation are presented in Table 2. In the present framework, regenerative braking efficiency η_{regen} is represented by an average effective parameter. In practice, this efficiency varies with parameters such as vehicle velocity, motor torque, battery state of charge, brake system pressure and the energy management strategy implemented by the vehicle manufacturer [29]. Since the objective of the proposed model is comparative route-level CO_2 assessment rather than detailed modeling of battery and motor control systems, an average efficiency was considered sufficient to capture the overall contribution of regenerative braking while maintaining computational simplicity. Accordingly, the present work adopts constant values consistent with experimentally reported average regenerative braking efficiencies for battery electric vehicles (approximately

60%) [30]. However, slightly different representative values (0.55–0.60) were adopted for the different vehicle categories, considering that more weight would slightly impact the efficiency [31,32]. The fuel and electricity parameters are presented in Table 3.

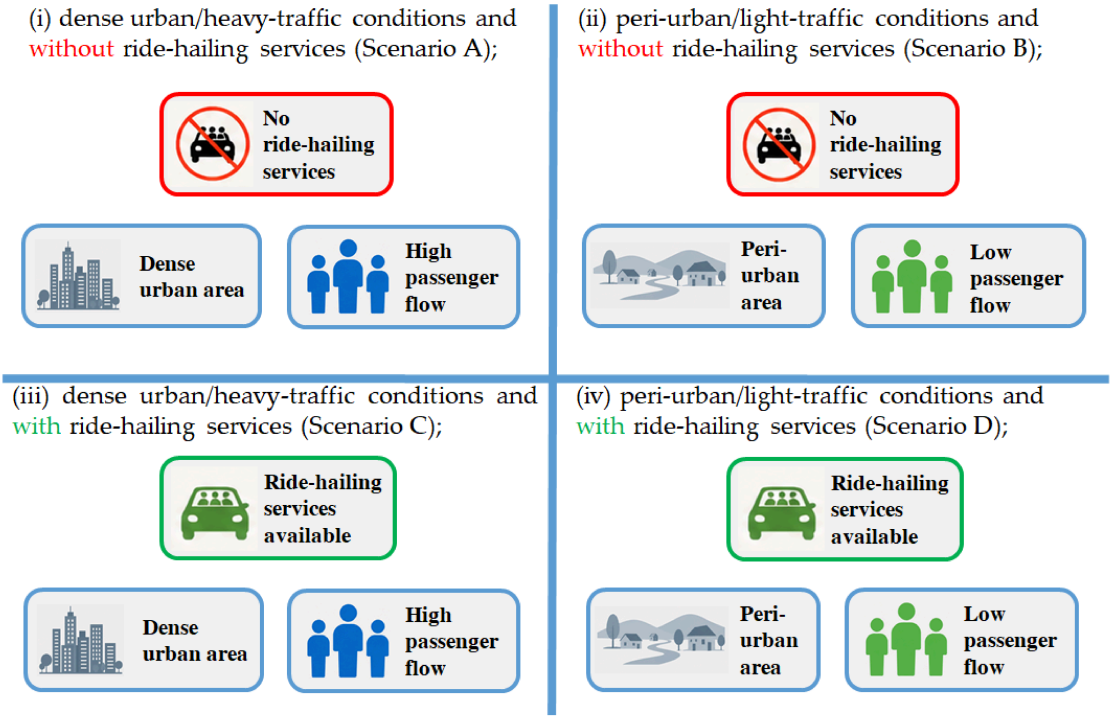


Figure 2. Graphical illustration of the simulation scenarios: (**i**) dense urban/heavy-traffic conditions and without ride-hailing services (Scenario A); (**ii**) peri-urban/light-traffic conditions and without ride-hailing services (Scenario B); (**iii**) dense urban/heavy-traffic conditions and with ride-hailing services (Scenario C); (**iv**) peri-urban/light-traffic conditions and with ride-hailing services (Scenario D).

Table 2. Vehicle parameters used in the simulation.

Vehicle	Powertrain	Mass m (kg)	C_d	Frontal Area A (m^2)	C_{rr}	Effective Average Powertrain Efficiency η	Regenerative Efficiency η_{regen}	Auxiliary Power P_{aux} (W)
Mini	Gasoline	1050	0.3	2.05	0.011	0.22	–	–
Mini	Diesel	1120	0.3	2.05	0.011	0.24	–	–
Mini	Electric	1300	0.29	2.05	0.011	0.88	0.6	450
Compact	Gasoline	1350	0.3	2.2	0.012	0.22	–	–
Compact	Diesel	1450	0.3	2.2	0.012	0.24	–	–
Compact	Electric	1600	0.29	2.2	0.012	0.88	0.55	600
SUV	Gasoline	1850	0.35	2.6	0.013	0.21	–	–
SUV	Diesel	1950	0.35	2.6	0.013	0.23	–	–
SUV	Electric	2200	0.33	2.6	0.013	0.86	0.6	700
Minibus	Diesel	3200	0.42	4	0.014	0.25	–	–
Minibus	Electric	3800	0.42	4	0.014	0.85	0.58	900
Bus	Diesel	11,500	0.55	7.5	0.015	0.28	–	–
Bus	Electric	13,000	0.55	7.5	0.015	0.83	0.55	1800

Note: "–" indicates that the value is not applicable.

Table 3. Fuel and electricity parameters.

Parameter	Gasoline	Diesel	Electricity
LHV (J/kg)	43×10^3	42.5	–
Fuel density (kg/L)	0.745	0.832	–
ε emission factor	2.31 (kg CO_2/L)	2.68 (kg CO_2/L)	0.40 (kg CO_2/kWh)
k_{W2T}	0.2	0.18	–
Idle consumption (l/h)	1.1	0.9	–

As it can be seen in Table 4, for the first two scenarios, different vehicle occupancy levels and vehicle classes (mini, compact, SUV, mini-bus, bus) were considered, allowing detailed comparisons between transport strategies. Usually, mini cars are only for one person in light demand, rarely being used with two persons, so the average occupancy is 1 to 1.3 persons per trip. Compact cars can have one person during low passenger demand and two persons when the passenger demand is very high, with an average of 1.1 to 1.4. In the same conditions, SUVs are assumed to carry between one and three persons, with an average of 1.2 to 1.5. Mini-buses can have 8 to 12 people, and buses, between 40 and 60 persons, depending on passenger demand. For Scenarios C and D, the passenger-car occupancy values were intentionally increased to represent hypothetical high-occupancy demand-responsive mobility configurations and to investigate the influence of improved vehicle utilization on CO_2 emissions per passenger-kilometer. These occupancy values are imposed scenario parameters rather than empirical estimates of average occupancy for specific ride-hailing platforms. They constitute conditional comparative scenarios used to evaluate how the matching between vehicle capacity and passenger demand influences transport-related CO_2 emissions. Accordingly, the resulting differences between passenger cars, minibuses, and buses are valid under the occupancy assumptions defined in Table 4.

Table 4. Traffic scenario parameters.

Parameter	Scenario A	Scenario B	Scenario C	Scenario D
Traffic conditions	Heavy	Light	Heavy	Light
Route length (km)	10	10	10	10
Total passengers to be transported	1000	1000	1000	1000
Mini occupancy (passengers per vehicle)	1.3	1	2	2
Compact occupancy (passengers per vehicle)	1.4	1.1	4	3
SUV occupancy (passengers per vehicle)	1.5	1.2	5	4
Minibus occupancy (passengers per vehicle)	12	8	10	8
Bus occupancy (passengers per vehicle)	60	40	50	25

To ensure a common basis for comparison, all simulations consider a fixed total of 1000 passengers requiring transportation over the same 10 km route, and the required number of vehicles for each category is calculated according to the assumed occupancy values. The number of 1000 passengers therefore represents a normalization basis for the comparative CO_2 assessment rather than a passenger-demand model. After that, the simulator estimates the CO_2 emissions for each scenario.

The speed–time profiles considered in this study are representative synthetic driving profiles developed for simulation purposes. They were designed to reproduce typical urban and peri-urban operating conditions while ensuring identical driving conditions for all vehicle categories evaluated. Consequently, the simulations focus on comparative assessment rather than on reproducing traffic conditions in a particular city or transport network. All profiles were generated for a route length of 10 km using a constant numerical time step of $\Delta t = 1$ s, while the road gradient was set to 0% for the scenarios investigated. Two traffic conditions were considered: light traffic, used in Scenarios B and D, and heavy traffic, used in Scenarios A and C. The corresponding generated profiles have mean speeds of approximately 30 km/h and 15 km/h and travel durations of 1200 s and 2400 s, respectively, while the maximum speeds are approximately 37.7 km/h and 39.5 km/h. The traffic conditions are differentiated not only by their mean speeds but also through the parameters of the stochastic speed-profile generator. Specifically, the probability of initiating a stop at each simulation step is 0.002 for light traffic and 0.015 for heavy traffic, while the corresponding stop-duration ranges are 3–12 s and 20–90 s. The stochastic acceleration distributions were parameterized with a mean of 0.90 m/s^2 and a standard deviation of 0.40 m/s^2 for light traffic, and with both a mean and a standard deviation of 0.55 m/s^2 for heavy traffic, together with greater speed variability under heavy traffic. These parameters result in substantially more pronounced stop-and-go operation under heavy traffic. For the generated profiles used in the simulations, the cumulative time below the adopted stop threshold of 0.5 m/s was approximately 1 s for light traffic and 1006 s for heavy traffic. For each traffic condition, the same generated speed–time trajectory was applied to all vehicle classes and powertrain technologies, thereby ensuring controlled comparative conditions in which differences in calculated energy consumption and CO_2 emissions result from vehicle and powertrain parameters rather than from different driving trajectories. These profiles should therefore be interpreted as controlled synthetic driving conditions developed for comparative scenario analysis rather than as measured traffic trajectories representative of a specific city or road network.

3.2. Simulation Results

The results presented in Figure 3 are expressed as specific W2W CO_2 emissions in g CO_2/passenger-km. For each vehicle category and scenario, the total W2W CO_2 emissions estimated for the 10 km route are normalized by the corresponding number of passengers transported and by the route distance. Consequently, the values shown in Figure 3 represent the CO_2 emissions associated with transporting one passenger over one kilometer under the vehicle occupancy and traffic assumptions defined for each scenario. The most important aspect that arises is that under conditions of low occupancy and long headways (typical in peri-urban or poorly served areas), conventional public transport can have higher per-passenger emissions than high-occupancy ride-hailing or demand-responsive vehicles. Specifically, in underutilization conditions, public transportation can have higher emissions per passenger-kilometer than small cars that are used efficiently. Thus, these results support the hypothesis that there are circumstances in which conventional public transport is less CO_2 efficient per passenger than optimized individual transport. In turn, this points out

the importance of passenger-demand predictions and accurate correlation between the estimated number of passengers and the optimal allocation of vehicle type.

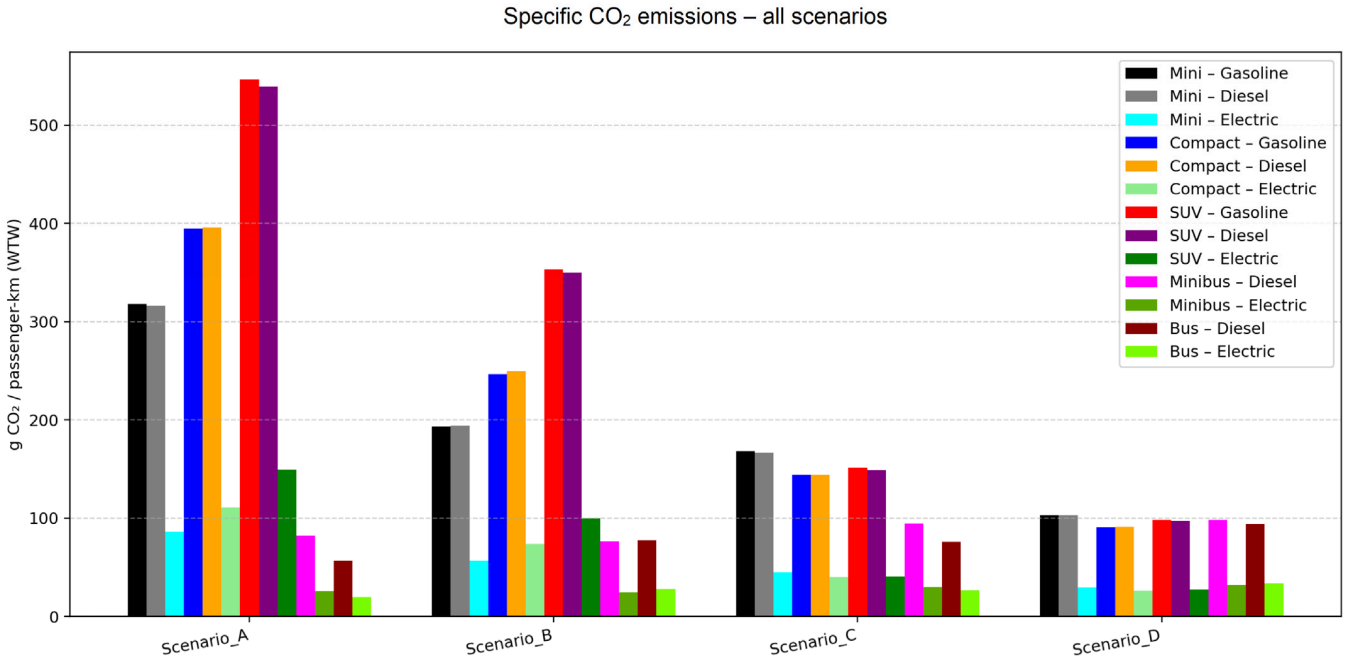


Figure 3. Estimated specific W2W CO_2 emissions (g CO_2/passenger-km) for the simulated 10 km route under Scenarios A–D.

The results also indicate that in peri-urban areas, where public transport occupancy is low, emissions of buses and minibuses can be comparable or even higher than those generated by electric cars in individual mode. This effect is accentuated in scenarios with low traffic and underuse of public transport vehicles, which is also supported by the literature in which population density plays a key role in the efficiency of transport modes.

Another important aspect that results from Figure 3 is a considerable decrease in specific CO_2 emissions when ride-hailing services increase vehicle occupancy. This trend is maintained for all passenger car categories, regardless of the propulsion technology. This demonstrates that vehicle occupancy has a stronger influence on emissions per passenger-kilometer than vehicle size. Within the passenger-car categories considered in this study (Mini, Compact, and SUV), increasing vehicle occupancy substantially reduces the specific CO_2 emissions per passenger-kilometer. Among these vehicle classes, SUVs exhibit the largest relative reduction because they experience the greatest relative increase in average occupancy between the simulated scenarios. Consequently, their percentage reduction in specific CO_2 emissions is larger than that observed for the Mini and Compact categories. This observation refers exclusively to the passenger-car classes analyzed in this study and should not be interpreted as a direct comparison with minibuses or buses, whose substantially higher baseline occupancies lead to different scaling behavior. The simulation results also show that EVs have the lowest specific emissions in all scenarios. Nevertheless, the results indicate again that occupancy remains an important factor even for low-emission propulsion technologies.

Another important aspect that results from Figure 2 is that no transport mode can be considered universally optimal from the perspective of CO_2 emissions. Instead, transportation environmental efficiency is obtained when vehicle capacity matches passenger demand. Next, other important factors are traffic conditions, population density, and vehicle occupancy. Consequently, the proposed CO_2 estimation framework provides a practical decision-support tool capable of identifying the most appropriate vehicle category for a given scenario. The

simulation results also show that conventional public transport is highly efficient in dense urban environments where high occupancy levels are ensured. Otherwise, its environmental performance decreases in peri-urban areas where occupancy gets lower.

The simulations suggest that in adaptive scenarios (ride-hailing), when vehicles are dynamically allocated based on real demand, total emissions can be reduced compared to classic non-demand-responsive public transport, especially in areas with dispersed demand. These results are in agreement with the literature suggesting the potential of integrated e-hailing services to reduce kilometers traveled and, implicitly, emissions generated [7].

Overall, these results show that adaptive demand-responsive mobility services can be a very effective complement to conventional public transport. Specifically, such ride-hailing services not only address specific user needs, but also represent a very efficient transport solution for areas characterized by low passenger demand and dispersed travel patterns.

4. Discussion

4.1. Interpretation of Results and Comparison with Previous Studies

What stands out clearly from the simulations is that vehicle occupancy has a major impact on specific CO_2 emissions per passenger-kilometer and this is not surprising. A vehicle requires energy to mainly overcome its mass, aerodynamic drag, rolling resistance, and uphill pass, while increasing the number of passengers would have a smaller contribution. Therefore, more people transported mean lower CO_2 emissions per passenger-kilometer. This is exactly the trend observed for all passenger car categories in this study.

The simulations also reveal a second important thing: the environmental performance is not determined by vehicle size alone. As the results show, large vehicles achieve their advantage only when they carry enough passengers. When the number of people transported decreases, the amount of energy required to move a large vehicle is shared among fewer passengers, leading to a rapid increase in emissions per passenger-kilometer. On the other hand, smaller vehicles can become efficient if they go with high occupancy rate when the demand is low. This does not mean that ride-hailing services are better than conventional public transportation. It only shows that the efficiency of any transportation mode depends on how well vehicle capacity matches passenger demand. This is consistent with findings of other studies. Empirical measurements on urban bus fleets have shown that the environmental benefit of public transportation depends on the number of passengers [33,34]. Therefore, the low-occupied buses can lose their environmental advantages relative to smaller passenger cars. Although the model presented in this paper studied four representative scenarios rather than specific transportation networks, the trends obtained in the simulations are well aligned with these real-world observations.

The simulations also suggest that ride-hailing services can be a good alternative in peri-urban areas, where travel demand is low and spread over a large area. However, it is necessary to take into account the context of the modeling assumptions adopted in this paper. The comparison does not explicitly include operational processes such as vehicle repositioning, deadheading between consecutive trips, or trip chaining. These additional activities increase the total distance traveled by ride-hailing vehicles relative to the number of passengers and may reduce their ecological advantage under real-world operating conditions. Therefore, the results should be interpreted as an illustration of the influence of occupancy rates and vehicle size, rather than as a universal comparison between transport modes.

4.2. Practical Implications

The present framework is intended to help decision-making in situations where various mobility solutions must be compared from a CO_2 emissions perspective. The

model does not promote one mode of transport over another. It simply takes into account vehicle category, occupancy rate, traffic conditions, and route characteristics to evaluate the environmental performance of passenger transportation. In planning strategies, the present proposal can also help identify the most appropriate vehicle category for a given transport demand, in order to match vehicle capacity with the estimated number of passengers. This observation can support the planning of ride-hailing services, especially in peri-urban areas where passenger demand is highly irregular throughout the day. The proposed methodology can also assist fleet operators evaluate different operational scenarios before implementation. For instance, changes in vehicle occupancy rates, route characteristics, or fleet composition can be analyzed to estimate their impact on W2W CO_2 emissions under the same modeling assumptions. Such analyses can help select the most efficient operational strategies for a specific transport service. Also, the proposal necessitates low computer power. The model requires only commonly available input data, such as vehicle characteristics, route information, and typical speed–time profiles. This would make it suitable for integration into decision-support applications. Another practical advantage is that the framework can be further extended without core modification when additional data sources become available.

4.3. Model Limitations and Future Development

Nevertheless, the proposed algorithm has some limitations. First, the model is deterministic and does not account for dynamic variations in traffic conditions. Second, the W2T component is represented using average emission factors, which may vary in certain conditions. In particular, the W2W results obtained for EVs depend on the electricity emission factor adopted in the analysis, which may vary according to the regional electricity-generation mix and the temporal characteristics of electricity production. Consequently, the EV-related results should be interpreted in relation to the electricity emission factor assumed in the present scenarios. Although the present work focuses on the development of a computationally efficient comparative assessment framework, future work can be further extended by dedicated sensitivity analyses to quantify the influence of weather conditions, auxiliary loads (e.g., HVAC operation), and unexpected traffic events on the estimated CO_2 emissions. Such analyses will support a more comprehensive evaluation of the robustness of the proposed methodology under real operating conditions. In addition, in the proposed algorithm, driver behavior is represented through predefined driving profiles rather than detailed individual driving characteristics. Furthermore, the proposed model considers only longitudinal vehicle dynamics. Consequently, additional energy losses associated with cornering resistance, tire slip, and steering maneuvers are not explicitly represented. Although these effects are generally smaller than the dominant longitudinal energy components, they may become more significant for highly sinuous urban routes and represent a natural direction for future model development. Also, idle fuel consumption is represented by a constant mass flow rate and does not explicitly account for automatic start–stop systems, accessory load variations, or engine thermal management. Although this approximation has only a limited influence, incorporating adaptive idle-consumption models constitutes an important direction for future work. Another approximation was for regenerative braking efficiency, which was represented by an average effective value. The present model therefore does not explicitly account for variations caused by battery state of charge, temperature, braking intensity, or control strategies. Another limitation is that the present framework estimates emissions generated during passenger transport only. Operational processes specific to ride-hailing services, including deadheading, vehicle repositioning between successive trips, and trip chaining, are not explicitly represented. Consequently, the total emissions associated with real-world ride-hailing operations may

be underestimated. Finally, the proposed method does not consider the effect of unexpected traffic events (i.e., accidents, road works, or temporary road closures). Despite these limitations, the proposed approach provides a computationally efficient framework for comparative analyses and decision support in transport planning and fleet management under the modelling assumptions adopted and considering passenger-carrying operation only.

Future work on the model will focus on increasing its accuracy and on further developing the practical applicability. In this direction, the first natural extension is the integration of real-time GPS trajectories and combination with live traffic information. This correlation between the two features of the RINO platform will enable dynamic emission estimation under continuously changing operating conditions, further improving the precision and enabling real-time management.

Another aspect should focus on the integration of Artificial Intelligence (AI) techniques for passenger demand prediction, vehicle allocation and route selection. In this perspective, AI integration is expected to improve the efficiency of demand-responsive mobility services.

5. Conclusions

The present study offers a computational framework for estimating W2W CO_2 emissions generated by different passenger transport modes. The proposed methodology takes into consideration vehicle dynamics, powertrain characteristics, route information, and occupancy for consistent comparisons among conventional passenger cars, public transportation, and demand-responsive mobility services.

The main conclusion is that simulations show that vehicle occupancy is one of the most important factors influencing specific CO_2 emissions per passenger-kilometer. The analysis also demonstrates that the environmental performance of a transportation mode cannot be evaluated independently of the operating conditions. Therefore, buses achieve their greatest benefit when passenger demand is sufficient, whereas smaller vehicles may become competitive in low-demand scenarios when the occupancy is high. These findings show the importance of matching vehicle capacity to actual passenger demand instead of assuming that one transportation mode is universally better. The results confirm empirical studies on real-world emissions of gaseous pollutants per passenger-kilometer traveled with various transportation modes.

The methodology relies on commonly available input data. Thus, it can support transport planning, fleet management, and scenario evaluation. Also, it can serve as the computational core of future ride-hailing platforms.

Finally, the proposed work should be viewed as a comparative decision-support methodology. The current implementation intentionally adopts several simplifications to ensure transparency and efficiency. Nevertheless, additional operational and environmental factors can be incorporated as new data become available, providing a flexible foundation for future developments in sustainable and demand-responsive mobility.

Author Contributions: Conceptualization, C.B. and A.-M.C.; methodology, C.B., A.-M.C., E.Z., A.L. and F.-M.S.; software, C.B., A.-M.C. and E.Z.; validation, C.B., A.-M.C., E.Z., S.-A.A., A.L. and F.-M.S.; formal analysis, C.B., A.-M.C., E.Z., S.-A.A. and A.L.; investigation, C.B. and A.-M.C.; resources, A.-M.C. and F.-M.S.; data curation, C.B., A.-M.C., E.Z. and S.-A.A.; writing—original draft preparation, C.B. and A.-M.C.; writing—review and editing, C.B., A.-M.C., E.Z., S.-A.A., A.L. and F.-M.S.; visualization, C.B., A.-M.C. and S.-A.A.; supervision, A.-M.C. and F.-M.S.; project administration, A.-M.C. and F.-M.S.; funding acquisition, A.-M.C. and F.-M.S. All authors have read and agreed to the published version of the manuscript.

Funding: This research was funded within the project "*AI-based IT Platform for Innovative and Sustainable Shared Mobility Solutions*" (SMIS Code: 338686), implemented by PROPTECH INDUSTRY S.R.L. as project leader. The project is funded through the *North-East Regional Programme 2021–2027*,

Priority PRNE_P1—*A more competitive and innovative region*, under the call *Support for strengthening the innovation capacity of SMEs through RDI projects and investments necessary for the development of innovative products and processes* (PR/NE/2024/P1/RSO1.1_RSO1.3/1).

Institutional Review Board Statement: Not applicable.

Informed Consent Statement: Not applicable.

Data Availability Statement: The original contributions presented in this study are included in the article. Further inquiries can be directed to the corresponding author.

Conflicts of Interest: Author Florinel-Mădălin Stoian was employed by the Proptech Industry. The remaining authors declare that the research was conducted in the absence of any commercial or financial relationships that could be construed as a potential conflict of interest.

Abbreviations

The following abbreviations are used in this manuscript:

ICEVs	Combustion Engine Vehicles
EVs	Electric Vehicles
MOVES	Motor Vehicle Emission Simulator
HBE-FA/PHEM	Handbook Emission Factors for Road Transport supported by Passenger Car and Heavy-Duty Employment Model
W2W	Well-to-Wheel
W2T	Well-to-Tank
T2W	Tank-to-Wheel
AI	Artificial Intelligence

References

1. Sivilevičius, H.; Žuraulis, V. Modeling the Impact of Interaction Factors for Transport System Elements on Quality of Life Using Multi-Criteria Decision-Making and Applied Statistical Methods. *Sustainability* **2025**, *17*, 1784. [CrossRef]
2. Mavlutova, I.; Atstaja, D.; Grasis, J.; Kuzmina, J.; Uvarova, I.; Roga, D. Urban Transportation Concept and Sustainable Urban Mobility in Smart Cities: A Review. *Energies* **2023**, *16*, 3585. [CrossRef]
3. World Health Organization (WHO). Road Traffic Injuries. 1 May 2026. Available online: https://www.who.int/news-room/fact-sheets/detail/road-traffic-injuries (accessed on 9 July 2026).
4. Ritchie, H. Which Form of Transport Has the Smallest Carbon Footprint? Our World in Data. 2023. Available online: https://archive.ourworldindata.org/20251125-173858/travel-carbon-footprint.html (accessed on 25 November 2025).
5. Liao, Y. Ride-sourcing compared to its public-transit alternative using big trip data. *J. Transp. Geogr.* **2021**, *95*, 103135. [CrossRef]
6. Lee, B.; Lee, S. Toward greener transit: Carbon-efficient density thresholds for public transit vs. private vehicles. *Transp. Res. Part D Transp. Environ.* **2025**, *140*, 104641. [CrossRef]
7. Tikoudis, I.; Martinez, L.; Farrow, K.; García Bouyssou, C.; Petrik, O.; Oueslati, W. Ridesharing services and urban transport CO2 emissions: Simulation-based evidence from 247 cities. *Transp. Res. D Transp. Environ.* **2021**, *97*, 102923. [CrossRef]
8. Chang, X.; Chen, B.Y.; Li, Q.; Cui, X.; Tang, L.; Liu, C. Estimating real-time traffic carbon dioxide emissions based on intelligent transportation system technologies. *IEEE Trans. Intell. Transp. Syst.* **2013**, *14*, 469–479. [CrossRef]
9. Yalçın, S.E. Estimation of CO2 emissions in transportation systems using artificial neural networks, machine learning, and deep learning: A comprehensive approach. *Systems* **2025**, *13*, 194. [CrossRef]
10. Jang, S.; Park, J.; Yu, G.; Hwang, J. Tools for estimating traffic emissions considering spatial scales and mitigation strategies: A systematic review. *Int. J. Sustain. Transp.* **2025**, *19*, 431–445. [CrossRef]
11. Beba, H.; Öztürk, Z. Investigation of road transport-based greenhouse gas prediction models and the use of intelligent transportation systems for emission reduction. *Sci. Rep.* **2026**, *16*, 394. [CrossRef] [PubMed]
12. Wang, G.; Wang, S.; Li, W.; Yang, H. What determines carbon emissions of multimodal travel? Insights from interpretable machine learning on mobility trajectory data. *Sustainability* **2025**, *17*, 6983. [CrossRef]
13. Beguni, C.; Căilean, A.-M.; Zadobrischi, E.; Avătămăniței, S.-A.; Lavric, A.; Stoian, F.-M. The Convergence of Artificial Intelligence and Public Policy in Shaping the Future of Ride-Hailing: A Review. *Smart Cities* **2026**, *9*, 40. [CrossRef]
14. Zhou, S.; Chen, J.; Wu, Z.; Qiu, Y. Electrification of Online Ride-Hailing Vehicles in China: Intention Modelling and Market Prediction. *Energies* **2021**, *14*, 7380. [CrossRef]

15. Das, V. Does Adoption of Ridehailing Result in More Frequent Sustainable Mobility Choices? An Investigation Based on the National Household Travel Survey (NHTS) 2017 Data. *Smart Cities* **2020**, *3*, 385–400. [CrossRef]
16. Etminani-Ghasrodashti, R.; Hamidi, S. Individuals' Demand for Ride-hailing Services: Investigating the Combined Effects of Attitudinal Factors, Land Use, and Travel Attributes on Demand for App-based Taxis in Tehran, Iran. *Sustainability* **2019**, *11*, 5755. [CrossRef]
17. Poliziani, C.; Hsueh, G.; Czerwinski, D.; Wenzel, T.; Needell, Z.; Laarabi, H.; Schweizer, J.; Rupi, F. Micro Transit Simulation of On-Demand Shuttles Based on Transit Data for First- and Last-Mile Connection. *ISPRS Int. J. Geo-Inf.* **2023**, *12*, 177. [CrossRef]
18. Agarwal, S.; Mani, D.; Telang, R. The impact of ride-hailing services on congestion: Evidence from Indian cities. *Manuf. Serv. Oper. Manag.* **2023**, *25*, 862–883. [CrossRef]
19. Anair, D.; Martin, J.; Pinto de Moura, M.C.; Goldman, J. *Ride-Hailing's Climate Risks: Steering a Growing Industry Toward a Clean Transportation Future—Methodology*; Union of Concerned Scientists: Cambridge, MA, USA, 2020. Available online: https://www.ucsusa.org/sites/default/files/2020-02/Ride-Hailings-Climate-Risks-Methodology_0.pdf (accessed on 4 July 2026).
20. Rodier, C.; Michaels, J. *The Effects of Ride-Hailing Services on Greenhouse Gas Emissions*; National Center for Sustainable Transportation, University of California, Davis: Davis, CA, USA, 2019. Available online: https://escholarship.org/uc/item/4vz52416 (accessed on 4 July 2026).
21. Martin, E.; Shaheen, S.; Wolfe, B. Environmental impacts of transportation network company (TNC)/ride-hailing services: Evaluating net vehicle miles traveled and greenhouse gas emission impacts within San Francisco, Los Angeles, and Washington, D.C. using survey and activity data. *Sustainability* **2024**, *16*, 7454. [CrossRef]
22. Chen, L.; Xu, S.; Chen, Y.; Feng, J.; Chen, Q. Carbon Emissions Prediction for Sustainable Regional Transportation Based on a Hybrid Deep Learning Model. *Sustainability* **2026**, *18*, 6999. [CrossRef]
23. Tietge, U.; Díaz, S.; Mock, P.; Bandivadekar, A.; Dornoff, J.; Ligterink, N. From Laboratory to Road: A 2018 Update of Official and Real-World Fuel Consumption and CO_2 Values for Passenger Cars in Europe; International Council on Clean Transportation (ICCT): TNO. 2019. Available online: https://theicct.org/sites/default/files/publications/Lab_to_Road_2018_corrected-jul2021.pdf (accessed on 4 July 2026).
24. Beckers, C.J.J.; Besselink, I.J.M.; Nijmeijer, H. Assessing the impact of cornering losses on the energy consumption of electric city buses. *Transp. Res. D Transp. Environ.* **2020**, *86*, 102360. [CrossRef]
25. Linton, C.; Grant-Muller, S.; Gale, W.F. Approaches and Techniques for Modelling CO_2 Emissions from Road Transport. *Transp. Rev.* **2015**, *35*, 533–553. [CrossRef]
26. National Research Council. *Cost, Effectiveness, and Deployment of Fuel Economy Technologies for Light-Duty Vehicles*; The National Academies Press: Washington, DC, USA, 2015. [CrossRef] [PubMed]
27. Solano-Araque, E.; Colin, G.; Cloarec, G.-M.; Ketfi-Cherif, A.; Chamaillard, Y. Determining vehicle acceleration from noisy non-uniformly sampled speed data for control purposes. *IFAC-PapersOnLine* **2019**, *52*, 66–71. [CrossRef]
28. Zhu, R.; Fu, Y.; Wang, L.; Hu, J.; He, L.; Wang, M.; Lai, Y.; Su, S. Effects of a start-stop system for gasoline direct injection vehicles on fuel consumption and particulate emissions in hot and cold environments. *Environ. Pollut.* **2022**, *308*, 119689. [CrossRef] [PubMed]
29. Szumska, E.M. Regenerative Braking Systems in Electric Vehicles: A Comprehensive Review of Design, Control Strategies, and Efficiency Challenges. *Energies* **2025**, *18*, 2422. [CrossRef]
30. Armenta-Déu, C.; Cortés, H. Analysis of Kinetic Energy Recovery Systems in Electric Vehicles. *Vehicles* **2023**, *5*, 387–403. [CrossRef]
31. Kivekäs, K.; Lajunen, A.; Vepsäläinen, J.; Tammi, K. City Bus Powertrain Comparison: Driving Cycle Variation and Passenger Load Sensitivity Analysis. *Energies* **2018**, *11*, 1755. [CrossRef]
32. Lee, G.; Song, J.; Han, J.; Lim, Y.; Park, S. Study on energy consumption characteristics of passenger electric vehicle according to the regenerative braking stages during real-world driving conditions. *Energy* **2023**, *283*, 128745. [CrossRef]
33. Soukhov, A.; Mohamed, M. Occupancy and GHG emissions: Thresholds for disruptive transportation modes and emerging technologies. *Transp. Res. D Transp. Environ.* **2022**, *102*, 103127. [CrossRef]
34. Dhital, N.B.; Wang, L.-C.; Yang, H.-H.; Lee, C.-H.; Shih, W.-H.; Wu, C.-S. Effects of the COVID-19 pandemic on public bus occupancy and real-world tailpipe emissions of gaseous pollutants per passenger kilometer traveled. *Sustain. Environ. Res.* **2022**, *32*, 35. [CrossRef]

Disclaimer/Publisher's Note: The statements, opinions and data contained in all publications are solely those of the individual author(s) and contributor(s) and not of MDPI and/or the editor(s). MDPI and/or the editor(s) disclaim responsibility for any injury to people or property resulting from any ideas, methods, instructions or products referred to in the content.